Bull. Mater. Sci., Vol. 28, No. 5, August 2005, pp. 487–493. © Indian Academy of Sciences.

# Studies on preparation and characterization of indium doped zinc oxide films by chemical spray deposition

**BENNY JOSEPH*, P K MANOJ[†] and V K VAIDYAN[†]**

Department of Physics, St. Joseph's College, Calicut 673 008, India
[†]Department of Physics, University of Kerala, Trivandrum 695 581, India

MS received 22 December 2004; revised 16 May 2005

**Abstract. The preparation of indium doped zinc oxide films is discussed. Variation of structural, electrical and optical properties of the films with zinc acetate concentration and indium concentration in the solution are investigated. XRD studies have shown a change in preferential orientation from (002) to (101) crystal plane with increase in indium dopant concentration. Films deposited at optimum conditions have a low resistivity of $1{\cdot}33 \times 10^{-4}$ Ωm with 94% transmittance at 550 nm. SEM studies have shown smooth polycrystalline morphology of the films. Figure of merit is evaluated from electrical resistivity and transmittance data.**

**Keywords. Zinc oxide; indium doping; spray pyrolysis; transparent conductors.**

## 1. Introduction

Zinc oxide (ZnO) is a multi functional material with a wide range of applications. ZnO films have attracted considerable attention because they can be made to have high electrical conductivity, high infrared reflectance and high visible transmittance. Low resistive zinc oxide films have been achieved by doping with different group III elements like aluminium, boron, indium, gallium or with group VII elements like fluorine (Chopra *et al* 1983). Many techniques including evaporation, chemical vapour deposition, spray pyrolysis, sputtering, etc can be employed to deposit these films (Roth and Williams 1981; Ohya *et al* 1996; Benny Joseph *et al* 1998; Berhanu *et al* 2003). For applications like solar cell fabrication, spray pyrolysis technique is well known for its simplicity and possibility to produce large area films. The properties of the deposited material can be varied and controlled by proper optimization of spraying conditions.

In spray pyrolysis technique, low resistive ZnO films are obtained either by post-deposition heat treatment in vacuum or by hydrogen atmosphere or by adding donor impurities such as aluminium or indium. In the present study, indium doped zinc oxide (IZO) films have been prepared by using spray pyrolysis technique. The effect of indium doping on the structural, electrical and optical properties of IZO films have been reported.

## 2. Experimental

Indium doped zinc oxide films were deposited on glass substrates using spray pyrolysis technique. The deposition method involves the decomposition of an aqueous solution of zinc acetate. To achieve indium doping, indium trichloride ($InCl_3$) was added to the solution. The In/Zn ratio was varied from zero to 1·6 at.%. The resulting solution was sprayed onto heated substrates held at 723 ± 5 K. The upper limit for dopant concentration was fixed at 1·6 at.%. Compressed air was used as the carrier gas. To enhance electrical conductivity, as-deposited films were annealed at 573 K for 90 min under a vacuum of $10^{-5}$ mbar. Films from zinc acetate solution having molarity, 0·2 and 0·4 M, were also deposited at optimum doping level keeping the other process parameters constant. The apparatus and the deposition details have already been reported (Benny Joseph *et al* 1999).

Thicknesses of the films were measured using the multiple beam interferometric technique (Tolansky 1948). The structure of the films was studied using Philips PW 1710 X-ray diffractometer (XRD) and the surface morphology using JEOL 35C scanning electron microscope (SEM). The optical transmission studies were carried out using a Shimadzu UV-240 double beam spectrophotometer in the range 300–900 nm. The resistivity of the film was measured using a four-probe set up.

## 3. Results and discussion

### 3.1 *XRD studies*

Figure 1 shows the X-ray diffraction patterns of IZO films with different indium concentrations deposited at a substrate temperature of 723 ± 5 K using 0·1 M zinc acetate solution. All the peaks in the pattern correspond to hexagonal structure of ZnO and are indexed on the basis of

*Author for correspondence
(benny_chellamkottu@rediffmail.com)

ASTM data card 5-664. No phase corresponding to indium/indium oxide or other indium compounds was detected in the XRD. Significant changes are observed in the X-ray diffraction patterns which have shown a decrease of peak intensity corresponding to (002) crystal plane and an increase of peak intensity corresponding to (101) crystal plane with increase of dopant concentration. Undoped zinc oxide films have exhibited preferential orientation along (002) crystal plane. A similar effect was reported in the literature (Krunks and Mellikov 1995) which has shown that 5 at.% indium doping will lead to the formation of films with preferential orientation along (101) crystal plane. Many researchers have also reported the attenuation of orientation along (002) crystal plane and an enhancement of orientation along (100) crystal plane with increase of indium dopant concentration (Cossement and Streydio 1985; Tiburcio–Silver *et al* 1991; Goyal *et al* 1992b; Messaoudi *et al* 1995). To describe the preferential orientation, the texture coefficient, *TC* (*hkl*), is calculated using the expression (Barret and Massalski 1980):

$$TC\,(hkl) = \frac{I(hkl)/I_0\,(hkl)}{N_r^{-1}\sum_{N_r} I\,(hkl)/I_0(hkl)}, \qquad (1)$$

where $I$ is the measured intensity, $I_0$ the ASTM standard intensity and $N_r$ the reflection number. The texture coefficient is calculated for the crystal planes (002) and (101). Figure 2 depicts the variation of *TC*(002) and *TC*(101) of ZnO films prepared using 0·1 M zinc acetate solution at 723 ± 5 K for different dopant concentrations. The texture coefficient along (002) crystal plane decreases and that along (101) crystal plane increases with indium dopant concentration. The physical properties of IZO films are also found to be optimum for the films doped with 0·8 at.% indium in the starting solution. The lattice constants calculated from the most prominent peaks and the relative intensity ratio, *I*(002)/*I*(101), in the diffraction patterns of zinc oxide films deposited under various doping levels are given in table 1. The lattice constants obtained are found to be in good agreement with ASTM data 5-664 of powder ZnO sample.

Figure 3 shows the X-ray diffraction patterns of 0·8 at.% indium doped zinc oxide films prepared at 723 ± 5 K using zinc acetate precursor solutions of different molarities. All the peaks in the diffraction patterns coincide well with the patterns observed for hexagonal structure of ZnO powder sample. All the films prepared at 0·8 at.% indium doping concentration exhibited *c*-axis orientation which is found to improve with an increase in molarity of the spraying solution. Figure 4 shows the variation of *TC*(002) and *TC*(101) with molarity of the precursor solution. The high *c*-axis orientation at higher

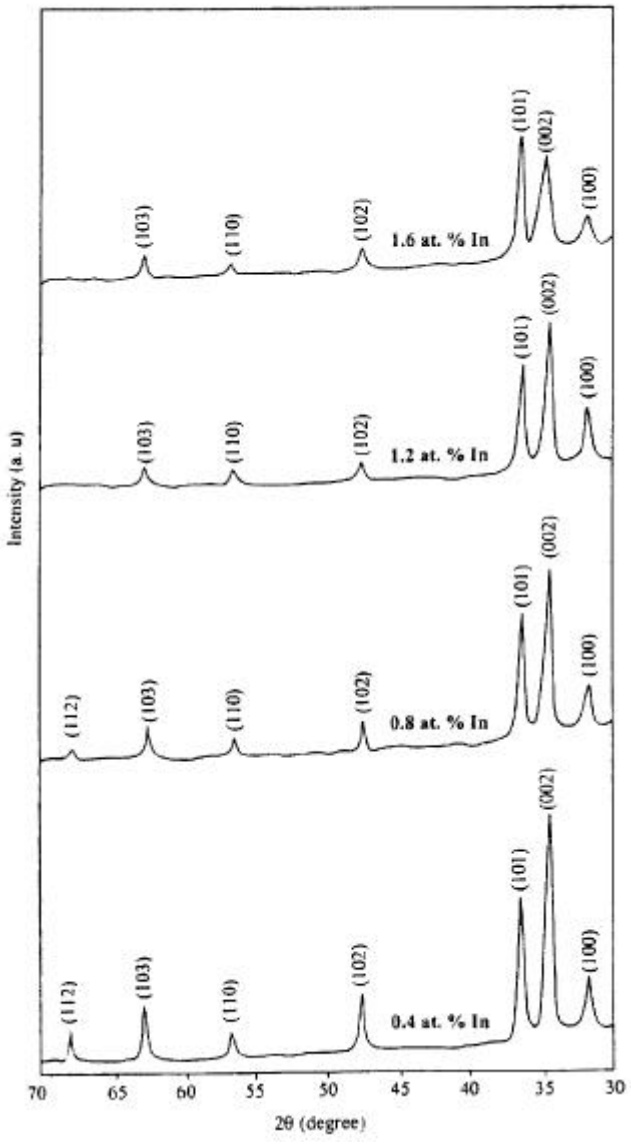


**Figure 1.** XRD patterns of IZO films deposited at 723 ± 5 K using 0·1 M zinc acetate solution with different indium concentrations.

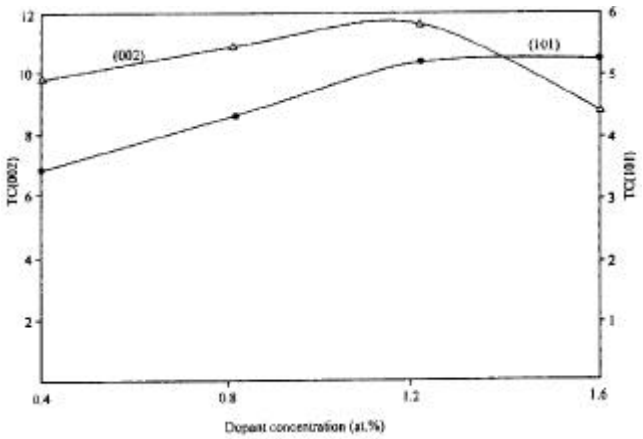


**Figure 2.** Variation of texture coefficient *TC*(002) and *TC*(101) of zinc oxide films deposited at 723 ± 5 K using 0·1 M zinc acetate solution with different indium concentrations.

molarity of the precursor solution is due to the combined effect of increase in Zn incorporation, increase in growth rate and reorientational effect (Goyal *et al* 1992a; Agashe and Major 1996). The lattice constants calculated from the most prominent peaks and the relative intensity ratios, $I(002)/I(101)$, in the diffraction patterns of IZO films deposited using zinc acetate precursor solutions of different molarities are given in table 2. The lattice constants calculated from the most prominent peaks are found to be in good agreement with ASTM values.

### 3.2 *SEM studies*

Figure 5 shows the scanning electron micrographs (SEM) of indium doped zinc oxide films deposited at $723 \pm 5$ K using zinc acetate solutions (0·1 M) with different indium dopant concentrations. Figure 5(a) shows the morphology of undoped zinc oxide films. The micrographs show uniform polycrystalline nature of the films. There is no significant change in morphology due to indium doping. It can be seen from figures 5(a) to (d) that the grain size decreased at 0·4 at.% indium doping level and then increased with increase in dopant concentration. Another fact observed is of some segregation in heavily doped films.

### 3.3 *Electrical and optical studies*

The high electrical conductivity found in semiconducting oxide film is largely due to high electron concentration resulting from (a) deviation from stoichiometry and (b) impurity doping effects. When indium, a third group element is doped in ZnO, $In^{+3}$ atoms substitute $Zn^{+2}$ atoms and act as donors.

If $y$ is the amount of indium incorporated in the ZnO lattice as $In^{+3}$ and considering the oxygen vacancies the material can be described as (Jin *et al* 1988)

$$Zn_{1-y}InO_{1-x}(V_{\ddot{O}})_x e_{2x} e_y, \qquad (2)$$

where $V_{\ddot{O}}$ denotes doubly charged oxygen vacancies and $e$ denotes electrons. Effective doping is achieved when

**Table 1.** Lattice constants and $I(002)/I(101)$ ratio of zinc oxide films deposited at 723 K using 0·1 M zinc acetate solution with different indium concentrations.

| Indium dopant concentration (at.%) | Lattice constants | | $I(002)/I(101)$ |
|---|---|---|---|
| | $a_0$ (nm) | $c_0$ (nm) | |
| 0·4 | 0·3247 | 0·5206 | 1·592 |
| 0·8 | 0·3253 | 0·5210 | 1·403 |
| 1·2 | 0·3251 | 0·5208 | 1·250 |
| 1·6 | 0·3261 | 0·5208 | 0·759 |
| ASTM | 0·3249 | 0·5205 | 0·560 |

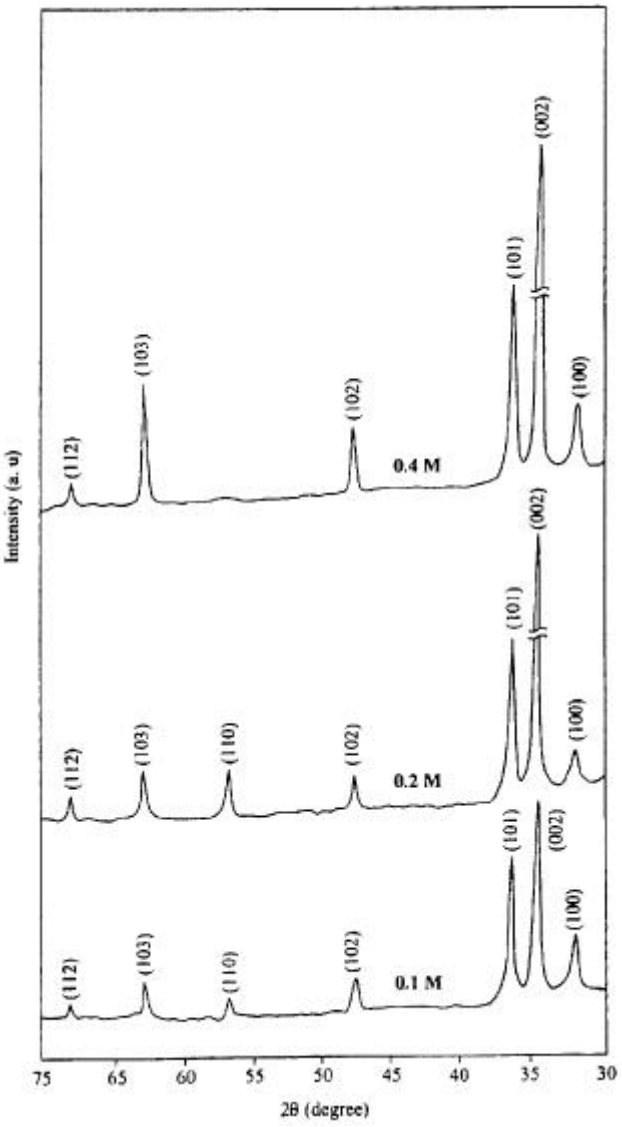


**Figure 3.** XRD patterns of 0·8 at.% indium doped zinc oxide films prepared at $723 \pm 5$ K using zinc acetate solutions of different molarities.

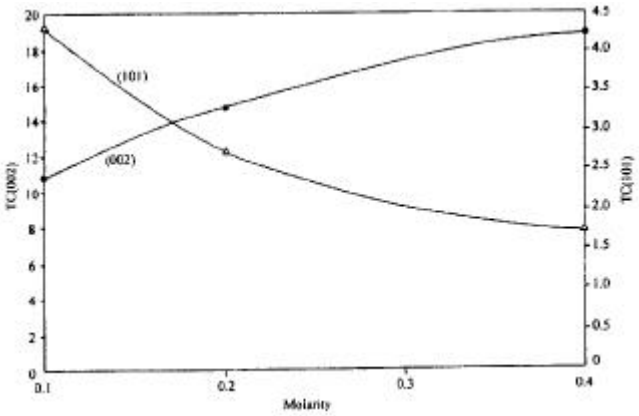


**Figure 4.** Variation of texture coefficient $TC(002)$ and $TC(101)$ of 0·8 at.% zinc oxide films deposited at $723 \pm 5$ K using zinc acetate solution of different molarities.

ionic radius of the dopant is same as or smaller than that of the host ion. The ionic radii of $Zn^{+2}$ and $In^{+3}$ are 0·074 and 0·081 nm, respectively.

The sheet resistance, resistivity, transmittance, optical bandgap and figure of merit of zinc oxide films prepared using 0·1 M zinc acetate solution for different dopant concentrations are given in table 3. The resistivities of as-deposited IZO films lie in the range $(1{\cdot}2–1{\cdot}75) \times 10^{-2}$ Ωm. Indium doping has reduced the resistivity of undoped films by two orders of magnitude. Since air and water were used as the carrier gas and solvent, respectively there is a possibility for chemisorption of oxygen during deposition of the films. Hence, the as-deposited films were annealed at 573 K for 90 min under a vacuum of $10^{-5}$ mbar to enhance the conductivity. Vacuum annealing yielded two orders of decrease of resistivity for IZO films. The low resistivity of IZO films is due to the combined effect of deviation from stoichiometry and doping. However, the resistivity increases at higher indium concentrations (> 0·8 at.%) and it may be due to the increase in disorder produced in the lattice. This increases the probability of scattering mechanism such as phonon scattering and ionized impurity scattering which are responsible for the increase in resistivity. Another possible explanation is that at higher concentrations, In segregates at grain boundaries in the form of $In(OH)_3$, hindering the electrical transport mechanism (Cossement and Streydio 1985). A minimum resistivity of $1{\cdot}33 \times 10^{-4}$ Ωm was obtained for films sprayed using 0·8 at% of indium in 0·1 M zinc acetate solution after vacuum annealing. The upper limit for doping concentration was fixed at 1·6 at% of indium as the films deposited at higher doping concentrations were of less transmittance.

**Table 2.** Lattice constants and relative intensity ratio $I(002)/I(101)$ of 0·8 at.% indium doped zinc oxide films deposited at 723 ± 5 K using zinc acetate solutions of different molarities.

| Molarity of solution (M) | Lattice constants | | $I(002)/I(101)$ |
|---|---|---|---|
| | $a_0$ (nm) | $c_0$ (nm) | |
| 0·1 | 0·3253 | 0·5210 | 1·403 |
| 0·2 | 0·3242 | 0·5202 | 2·999 |
| 0·4 | 0·3245 | 0·5200 | 6·154 |
| ASTM | 0·3249 | 0·5205 | 0·560 |

The sheet resistance, resistivity, transmittance, optical bandgap and figure of merit of 0·8 at% indium doped zinc oxide films prepared at substrate temperature, 723 ± 5 K, using precursor solutions of different molarities are given

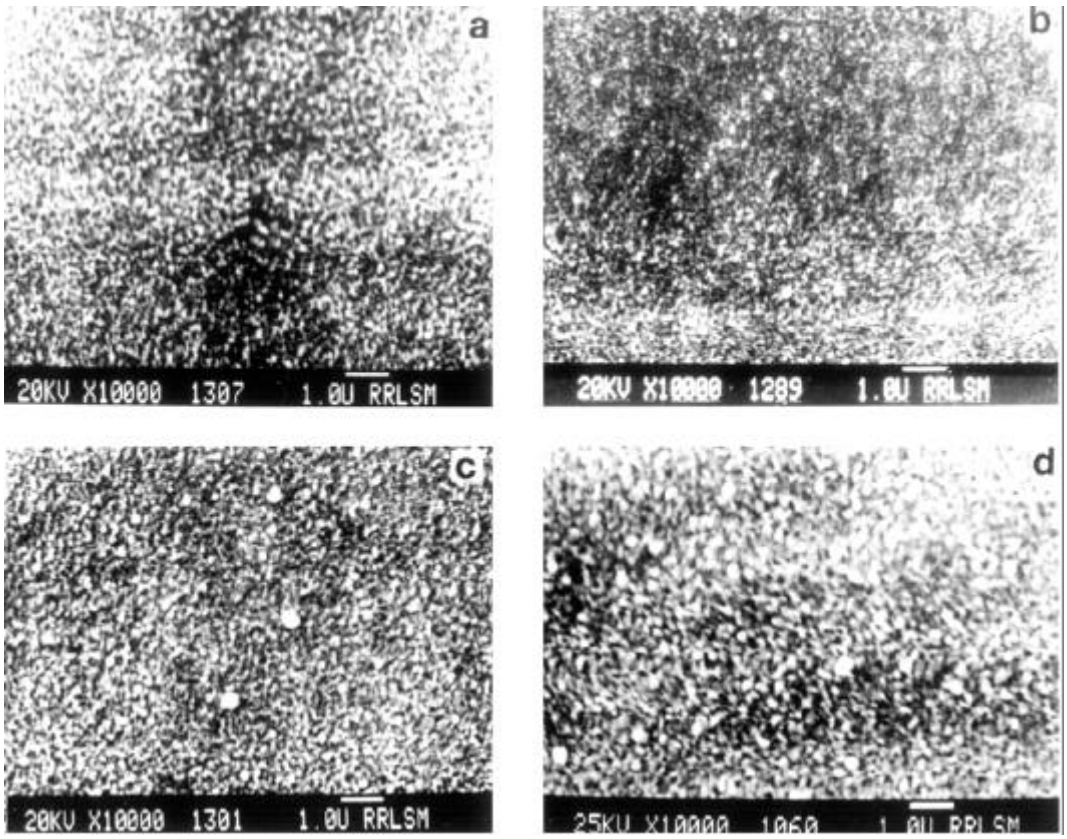


**Figure 5.** SEM photographs of IZO films deposited at 723 ± 5 K using 0·1 M zinc acetate solution with different indium concentrations: **a.** 0, **b.** 0·4 at.%, **c.** 1·2 at.% and **d.** 1·6 at.%.

**Table 3.** Electrical and optical properties of zinc oxide films (≈ 175 nm thickness) prepared at 723 ± 5 K using 0·1 M zinc acetate solutions with different indium dopant concentrations.

| Indium dopant concentrations (at.%) | Sheet resistance before annealing ($\times 10^3 \Omega/\square$) | Resistivity before annealing ($\Omega$m) | Sheet resistance after vacuum annealing ($\times 10^3 \Omega/\square$) | Resistivity after vacuum annealing ($\Omega$m) | Transmittance at 550 mm (%) | Optical bandgap (eV) | Figure of merit ($\Omega^{-1}$) |
|---|---|---|---|---|---|---|---|
| 0 | 9000 | 1·58 | 18 | $3{\cdot}15 \times 10^{-3}$ | 98 | 3·24 | $4{\cdot}5 \times 10^{-5}$ |
| 0·4 | 95 | $1{\cdot}66 \times 10^{-2}$ | 1·78 | $3{\cdot}12 \times 10^{-4}$ | 96 | 3·26 | $3{\cdot}7 \times 10^{-4}$ |
| 0·8 | 70 | $1{\cdot}23 \times 10^{-2}$ | 0·76 | $1{\cdot}33 \times 10^{-4}$ | 94 | 3·27 | $7{\cdot}1 \times 10^{-4}$ |
| 1·2 | 100 | $1{\cdot}75 \times 10^{-2}$ | 1·50 | $2{\cdot}63 \times 10^{-4}$ | 86 | 3·27 | $1{\cdot}5 \times 10^{-4}$ |
| 1·6 | 100 | $1{\cdot}75 \times 10^{-2}$ | 1·55 | $2{\cdot}71 \times 10^{-4}$ | 70 | 3·28 | $1{\cdot}8 \times 10^{-5}$ |

**Table 4.** Electrical and optical properties of IZO films deposited at 723 ± 5 K using 0·8 at% In doped zinc acetate solutions having different molarities.

| Molarity of solution (M) | Thick-ness (nm) | Sheet resistance before annealing ($\times 10^3\ \Omega/\square$) | Resistivity before annealing ($\Omega$m) | Sheet resistance after vacuum annealing ($\times 10^3\ \Omega/\square$) | Resistivity after vaccum annealing ($\Omega$m) | Transmi-ttance at 550 nm (%) | Optical bandgap (eV) | Figure of merit ($\Omega^{-1}$) |
|---|---|---|---|---|---|---|---|---|
| 0·1 | 175 | 70 | $1{\cdot}23 \times 10^{-2}$ | 0·76 | $1{\cdot}33 \times 10^{-4}$ | 94 | 3·27 | $7{\cdot}1 \times 10^{-4}$ |
| 0·2 | 300 | 55 | $1{\cdot}65 \times 10^{-2}$ | 0·40 | $1{\cdot}20 \times 10^{-4}$ | 80 | 3·29 | $2{\cdot}7 \times 10^{-4}$ |
| 0·4 | 450 | 34 | $1{\cdot}53 \times 10^{-2}$ | 0·26 | $1{\cdot}17 \times 10^{-4}$ | 76 | 3·29 | $2{\cdot}5 \times 10^{-4}$ |

in table 4. The film growth rate increased with concentration of the spraying solutions. Due to the high growth rate other atmospheric impurity contamination is expected to be lower, and incorporation of zinc at interstitial sites is expected to be greater (Goyal *et al* 1992a). Here the films of increasing thickness include the effects of increasing In incorporation, increasing growth rate as well as reorientational effects. This increases the carrier concentration and hence the resistivity decreases.

Figure 6 shows the optical transmission spectra of zinc oxide films prepared at substrate temperature, 723 ± 5 K, for different indium concentrations. The high transmittance of the films is a direct consequence of the wide bandgap. The transmittance is found to decrease at 1·2 at.% indium doping concentration. The decrease of transmittance at higher doping concentrations may be due to the increased scattering of photons by crystal defects created by doping. The free carrier absorption of photons may also contribute to the reduction in optical transmittance (Upadhyay *et al* 1989). The absorption coefficient is calculated from the transmission spectrum using the relation,

$$a = \ln(1/T)/t, \tag{3}$$

where $T$ is the transmittance and $t$ the thickness of the film. The optical bandgap of the films were calculated from $(\alpha h\nu)^2$ vs $h\nu$ graph. Figure 7 shows the typical variation of $(\alpha h\nu)^2$ vs $h\nu$ for 0·8 at.% indium doped zinc oxide film deposited at 723 ± 5 K using 0·1 M zinc acetate solution. The optical bandgap has increased from 3·24 to 3·28 eV with indium doping concentration from zero to 1·6 at%. The change in the optical bandgap can be explained in terms of Burstein–Moss bandgap widening

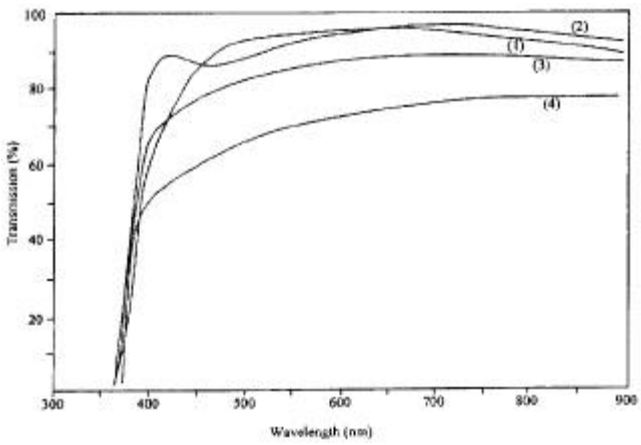


**Figure 6.** Optical transmission spectra of indium doped zinc oxide films deposited at a substrate temperature of 723 ± 5 K using 0·1 M zinc acetate solution for different indium concentrations: (1) 0, (2) 0·4 at.%, (3) 1·2 at.% and (4) 1·6 at.%.

and bandgap narrowing due to electron–electron and electron–impurity scattering (Burstein 1954; Moss 1954; Arai 1960; Mahan 1980; Berggren and Sernelius 1981). Figure 8 shows the transmission spectra of 0·8 at% indium doped zinc oxide films deposited at substrate temperature, 723 ± 5 K, using zinc acetate precursor solutions of different molarity. The decrease in transmittance at higher molarities may be due to the increase in thickness of the films. The optical bandgap was found to be ~ 3·29 eV for films deposited using precursor solutions of molarity 0·2 and 0·4 M.

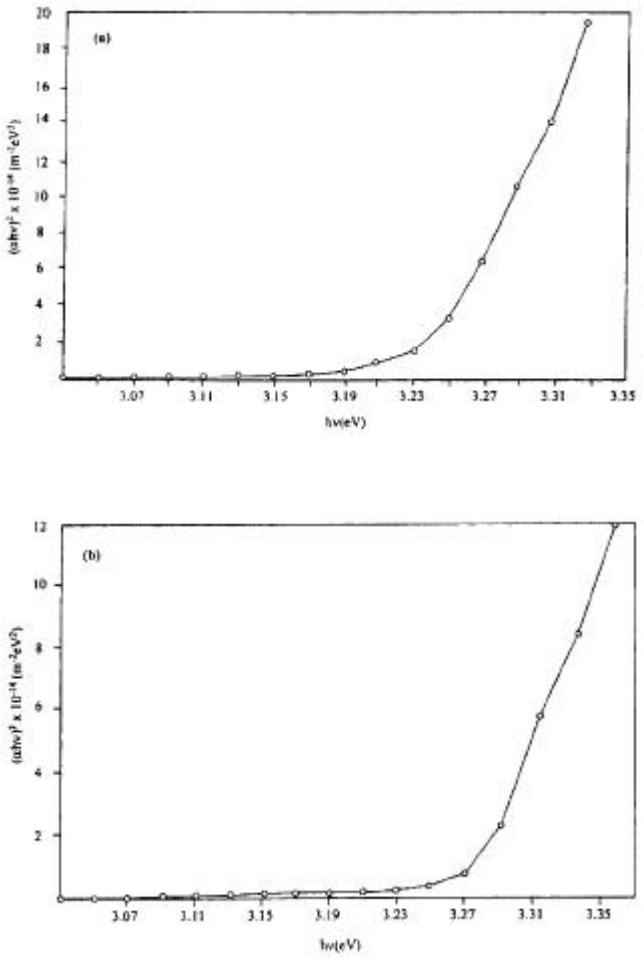


**Figure 7.** Typical variation of $(ahv)^2$ vs $hv$ of zinc oxide films deposited at $723 \pm 5$ K using 0·1 M zinc acetate solution with different indium doping concentrations (**a**) 0 and (**b**) 0·8 at.%.

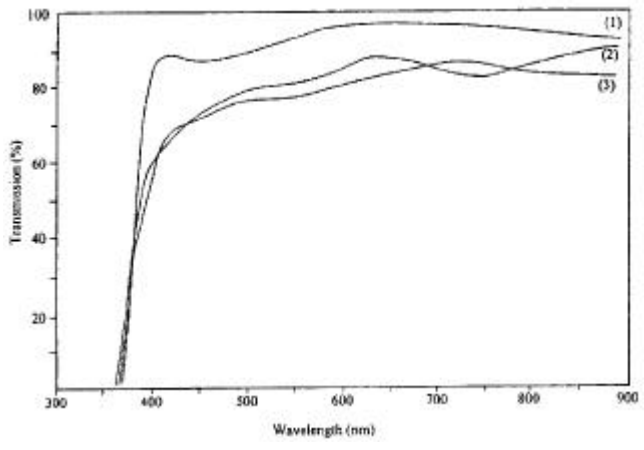


**Figure 8.** Optical transmission spectra of 0·8 at.% indium doped zinc oxide films deposited at a substrate temperature of $723 \pm 5$ K using zinc acetate solutions of different molarities: (1) 0·1, (2) 0·2 and (3) 0·4 M.

**Table 5.** Optimum spray conditions for the deposition of indium doped zinc oxide films.

| Spray parameter | Optimum value/item |
|---|---|
| Zinc acetate solution concentration | 0·1 M |
| Solvent | Distilled water |
| Substrate temperature | $723 \pm 5$ K |
| Carrier gas | Compressed air |
| Solution spray rate | 5–6 ml/min |
| In/Zn dopant ratio | 0·8 at% |
| Angular substrate to nozzle distance | $44 \pm 1$ cm |

The figure of merit of the films was calculated using the relation

$$f_{TC} = T^{10}/R_{\square}. \quad (4)$$

where $T$ is the transmittance, $R_{\square}$ the sheet resistance. The highest figure of merit obtained is $7{\cdot}1 \times 10^{-4}\ \Omega^{-1}$ for 0·8 at% indium doped films prepared using 0·1 M zinc acetate precursor solution. Table 5 gives the optimum conditions for the spray deposition of IZO films. In the present study, IZO films deposited under optimum conditions, have shown a low resistivity of $1{\cdot}33 \times 10^{-4}\ \Omega$m along with an optical transmittance of 94% at 550 nm.

## 4. Conclusions

Good quality IZO films were deposited using the spray pyrolysis method. The spray deposition of 0·8 at% indium doped zinc acetate (0·1 M) solution at substrate temperature $723 \pm 5$ K is found to be optimum for deposition of good quality films at the specified spray conditions. The films deposited at optimum conditions gave a transmittance of 94% at 550 nm and a low resistivity of $1{\cdot}33 \times 10^{-4}\ \Omega$m. Indium is suitable for preparing films with large figure of merit. SEM studies have revealed polycrystalline morphology of the films.

## References

Agashe C and Major S S 1996 in *Thin film characterization and applications* (eds) K Narayanadass and D Mangalraj (New Delhi: Allied Publishers)

Arai I 1960 *J. Phys. Soc. Jpn* **15** 916

Barret C and Massalki T B 1980 *Structure of metals* (Oxford: Pergamon)

Benny Joseph, Gopchandran K G, Manoj P K, Abraham J T, Peter Koshy and Vaidyan V K 1998 *Indian J. Phys.* **A72** 99

Benny Joseph, Gopchandran K G, Thomas P V, Peter Koshy and Vaidyan V K 1999 *Mater. Chem. Phys.* **58** 71

Berggren K F and Sernelius B E 1981 *Phys. Rev.* **B24** 1971

Berhanu D, Boyle D S, Govender K and O'Brien P 2003 *J. Mater. Sci.: Mater. Elect.* **14** 579

Burstein E 1954 *Phys. Rev.* **93** 638

Chopra K L, Major S and Pandya D K 1983 *Thin Solid Films* **102** 1

Cossement D and Streydio J M 1985 *J. Cryst. Growth* **72** 57
Goyal D J, Agashe C, Takwale M G, Marathe B R and Bhide B G 1992a *J. Mater. Sci.* **27** 4705
Goyal D J, Agashe C, Takwale M G, Marathe B R and Bhide B G 1992b *J. Mater. Sci. Lett.* **11** 708
Jin Z C, Hamberg I and Granqvist C G 1988 *J. Appl. Phys.* **64** 5117
Krunks M and Mellikov E 1995 *Thin Solid Films* **270** 33
Mahan G D 1980 *J. Appl. Phys.* **51** 2634
Messaoudi C, Sayah D and Abd-Lefdil M 1995 *Phys. Status Solidi* **(a)151** 93
Moss T S 1954 *Proc. Phys. Soc. London. Ser.* **B67** 775
Ohya Yutaka, Saiki Hisao, Tanaka Toshimasa and Takahashi Yasutaka 1996 *J. Am. Ceram. Soc.* **79** 825
Roth A P and Williams D F 1981 *J. Electrochem. Soc.* **128** 2684
Tolansky S 1948 *Multiple beam interferometry of surfaces and films* (London: Oxford University Press)
Tiburcio–Silver A, Joubert J C and Labeau M 1991 *Thin Solid Films* **197** 195
Upadhyay J P, Vishwakarma S R and Prasad H C 1989 *Thin Solid Films* **109** 195